Epidemic Model-Based Evaluation of Message Delivery Ratio of Probabilistic Flooding in Broadcast Communications

Shuji Kobayashi, Katsumi Sakakibara, and Jumpei Taketsugu

***Abstract*—A flooding mechanism is commonly employed in broadcast communications, where a node transfers a received message to its neighboring nodes upon its first reception. In order to mitigate the broadcast storm problem, probabilistic flooding has been proposed, where a message is transferred in a probabilistic manner. The contribution of this paper is to evaluate the temporal message delivery ratio in the probabilistic flooding. We first model the probabilistic flooding based on an epidemic model. Then, difference equations with respect to the number of nodes classified into three states are derived. We introduce the concept of the virtual radius, assuming that the spread of the message is annular. Finally, we evaluate the message delivery ratio as a function of the hop index. We validate the derived expressions by means of extensive computer simulation, assuming nodes are randomly dispersed in a square area. Numerical results indicate that the derived expressions are sufficiently accurate, when the product of the node density and the forwarding probability is greater than approximately two.**

***Index Terms*—Broadcast communications, Epidemic model, Message delivery ratio, Probabilistic flooding**

I. Introduction

BORDCASTING a message to all nodes in a network is one of primal and mandatory techniques in wireless ad-hoc and sensor networks [1][2]. For example, in AODV (Ad-hoc On-demand Distance Vector) routing protocol, a RREQ (Route REQuest) message is broadcast to start route discovery [3]. In VANETs (Vehicular Ad-hoc NETworks), safety-related information should be rapidly forwarded and shared in all vehicles near a originated vehicle [4].

To implement a broadcast mechanism, flooding is the simplest technique, where a node always forwards the message to be broadcast to its neighboring nodes upon its first reception. However, it is well-known that simple plain flooding results in the so-called broadcast storm problem [5], since it unfortunately brings forth a large amount of redundant traffic which may fatally break down the network. For the purpose of alleviation of the broadcast storm problem by deleting redundant traffic, a number of techniques have been proposed. Ni et al. [5] investigated probabilistic, counter-based and location-based schemes. In probabilistic flooding, a node rebroadcasts the message with probability p. The probability p is referred to as the forwarding probability. The possible message delivery ratio of probabilistic flooding is elaborately investigated in [6] in conjunction with the graph theory. Vakulya and Simon [7] modified probabilistic flooding, such that the forwarding probability at each node is determined as a function of the number of its neighboring nodes. The final message delivery ratio was then examined by extensive computer simulation. Qayyum et al. [8] introduced the concept of multipoint relaying, in which each node heuristically selects a subset of neighbors which will cover all two-hop neighbors.

In evaluating broadcast mechanisms, not only the final message delivery ratio but also the temporal speed of message dissemination are important performance measure. Since a broadcast mechanism should be designed so as to achieve the desired message delivery ratio within a predefined time interval, it is inevitable to evaluate temporal behavior of the spread of a broadcast message. Unfortunately, however, in the above literature [4]–[8] the authors pay their attention only to analyze the final message delivery ratio.

In this context, an epidemic model [9] is suitable for investigating how fast the message is disseminated in the network. From the viewpoint of infection prophylaxis, mathematical modeling of infectious diseases is a important tool to investigate the mechanisms for outbreak and the spread of diseases. An epidemic model enables us to predict the future course in order to control an epidemic. Therefore, it is reasonable to employ an epidemic model in analyzing time-scale behavior of a broadcast protocol. In general, an epidemic model consists of a system of differential equations with respect to the number or the ratio of susceptible, infected, and recovered individuals. These equations include the infection rate and the removal rate as parameters. In [10][11],

Manuscript received March 4, 2013.

Shuji Kobayashi is with the Department of Information and Communication Engineering, Faculty of Computer Science and System Engineering, Okayama Prefectural University, Soja, 719-1197 Japan. (e-mail: s-koba@c.oka-pu.ac.jp).

Katsumi Sakakibara is with the Department of Information and Communication Engineering, Faculty of Computer Science and System Engineering, Okayama Prefectural University, Soja, 719-1197 Japan. (phone: +81-866-94-2109; Fax: +81-866-94-2199; e-mail: sakaki@c.oka-pu.ac.jp).

Jumpei Taketsugu is with the Department of Information and Communication Engineering, Faculty of Computer Science and System Engineering, Okayama Prefectural University, Soja, 719-1197 Japan. (e-mail: taketugu@c.oka-pu.ac.jp).

the propagation of virus or malware in a wireless sensor network is analyzed adopting differential equations derived in an epidemic theory. The analysis by De et al. [10] is carried out by assuming that the infection rate and the removal rate are time-invariant. They also assume that virus is spread annularly in a network, which may be valid for a dense network. Tang et al. [11] also assume the constant infection and removal rates. However, these rates may be time-variant in a network where nodes are dispersed in a bounded region, since less forwarding may happen when the broadcast message reaches to nodes located in the vicinity of the boundary.

In this paper, we analyze the temporal message delivery ratio of probabilistic flooding in a network where nodes are randomly deployed in a square region. The analysis is based on an epidemic model with the annular spread assumption. However, we modify the model by taking into account the forwarding probability and by introducing the concept of the virtual radius, so that the annular spread assumption can be applied to a network of moderate-density. Then, we examine the accuracy of the derived expressions by means of extensive computer simulation.

The remainder of this paper is organized as follows: In Section II, we briefly review an epidemic model and then a model for probabilistic flooding is constructed. Section III presents the analysis of the time-scale message delivery ratio in a network consisting of nodes dispersed in a square region. Numerical results are given in Section IV to examine the accuracy of the model. Section V concludes the present paper.

II. PRELIMINARIES

A. Epidemic Models [9]

An epidemic model has been developed in order to gain insights into mechanisms influencing disease spread and to link individual-scale clinical knowledge with population-scale patterns. With the aid of an epidemic model, we can estimate behavior of infectious disease temporally and predict how many people will be infected by an infectious disease and when it will cease to spread. According to consideration to the feasibility of re-infection, the incubation period and other clinical characteristics of infectious disease to be modeled, an epidemic mode is classified into some categories, for instance, SI (Susceptible-Infectious) model, SIS (Susceptible-Infectious-Susceptible) model, SIR (Susceptible-Infectious-Recovered) model, and SEIR (Susceptible-pre-infectious-Infectious-Recovered) model. Among them, taking into account the state transition of a node in probabilistic flooding, we focus on SIR model.

In SIR model, an individual is in either of State S (Susceptible), State I (Infected) or State R (Recovered) at any time. An individual in State S transits into State I, if he or she occasionally contacts with any of the infectious individuals.

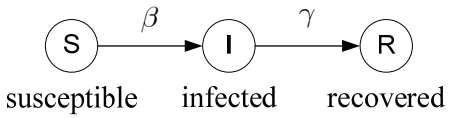

Fig. 1. State transition of an individual in SIR model

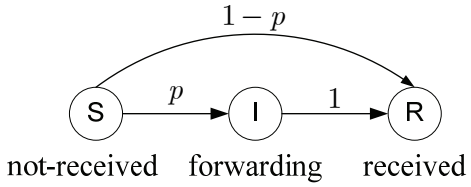

Fig. 2. State transition of a node in probabilistic flooding

An infectious individual becomes recovered after a while and a recovered individual gains immunity against the infectious disease. The state transitions of a individual in SIR model is illustrated in Fig. 1, where β and γ denote the infection rate and the removal rate, respectively. With these notations, the number of individuals in each state can be approximately obtained by solving a system of differential equations;

$$\begin{cases} \dfrac{dS(t)}{dt} = -\beta S(t) I(t), \\ \dfrac{dI(t)}{dt} = \beta S(t) I(t) - \gamma I(t), \\ \dfrac{dR(t)}{dt} = \gamma I(t), \end{cases} \tag{1}$$

where $S(t)$, $I(t)$, and $R(t)$ represent the number of individuals at time t in State S, State I, and State R, respectively. Here, if the total population is constant N , that is, if no one is born and no one dies, the relation $S(t) + I(t) + R(t) = N$ holds for any $t \geq 0$.

B. Modeling of Probabilistic Flooding

In probabilistic flooding, each node decides whether or not to transfer a received message to its neighboring nodes in a probabilistic manner, if it is the first reception [5][6]. Compared to the plain flooding, the probabilistic flooding can reduce the amount of redundant message forwarding in the network, which can mitigate the broadcast storm problem. Nodes can be classified into three categories; that is, (i) a node which has not received the broadcast message, (ii) a node which is just forwarding the message to its neighbors, and (iii) a node which has already received the message. Fortunately, these three states of a node can be associated with State S, State I and State R in SIR model shown in Fig. 1.

Let p denote the forwarding probability. Then, the state transition of a node can be depicted as shown in Fig. 2. A node

in State S moves to State I with probability p upon reception of the message and to State R with probability $1-p$. After forwarding the message, a node in State I goes to State R. Note that a node in State S directly moves into State R in the probabilistic flooding, if it chooses not to transfer the message. Note that State R is an absorbing state, since no nodes in State R rebroadcast the message thereafter.

III. Message Delivery Ratio

A. System Model and Assumptions

Suppose a network consisting of N nodes with transmission range r_0. We locate one source node at the origin on a two-dimensional plane and randomly disperse other $N-1$ nodes in a square region with side L, as shown in Fig. 3. The node density is given by

$$\sigma = \frac{N}{L^2}. \tag{2}$$

In order to make the analysis mathematically tractable, we impose the following assumptions.

A) No nodes join and leave the network during message dissemination. Hence, the total number of nodes, N, is constant. All nodes are geographically stable, that is, the positions of nodes are also time-invariant (stable network assumption).

B) A new message to be broadcast is transmitted at the source node at $t = 0$ and no other new messages are generated by any nodes afterward.

C) The forwarding probability p and the transmission range r_0 are identical for all nodes (homogeneous node assumption).

D) A node can receive one or more broadcast messages simultaneously, that is, no destructive message collisions occur at a receiving node.

E) Channels between nodes are error-free.

From Assumption C), each node connects with $\pi r_0^2 \sigma$ nodes on the average. Assumptions D) and E) enable us to perceive that a node can receive one or multiple forwarded messages correctly, if it is located within the transmission range of one or more forwarding nodes, that is, nodes in State I. With the aid of the above assumptions, the probabilistic flooding can be described by a discrete-time process with unit time of the message duration. It implies that the message is forwarded in a hop-by-hop manner.

Let t be a non-negative integer representing the hop index. At $t = 0$ the source node is in State I and other node are in State S. The source node moves to State R at $t = 1$. Nodes within the transmission range of the source node become State I with probability p or State R with probability $1-p$ at $t = 1$, as shown in Fig. 2.

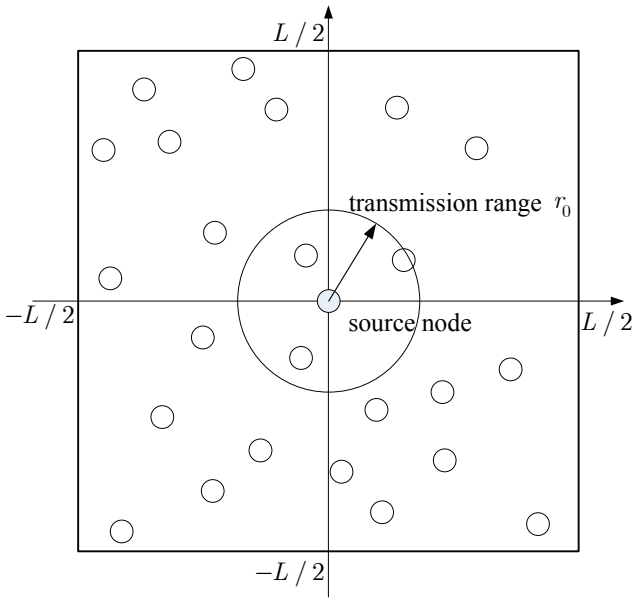

Fig. 3. Network configuration with one source node located at the origin and other nodes dispersed in a square region with side L.

B. Difference Equations and Message Delivery Ratio

Let $S(t)$, $I(t)$, and $R(t)$ denote the number of nodes in State S, State I and State R at the end of the t th hop, respectively. It follows Assumption A) that the relation $S(t)+I(t)+R(t)=N$ holds for any $t = 0,1,2,...$ similarly to the epidemic model in Section II.A. Clearly,

$$S(0) = N-1, \quad I(0) = 1, \quad R(0) = 0. \tag{3}$$

We denote by $A(t)$ an area where a broadcast message is newly delivered at the t th hop, that is, a node in $A(t)$ turns from State S to either of State I or State R. It is clear that $A(1) = \pi r_0^2$, if $r_0 \le L/2$. The average number of nodes in $A(t)$ is $\sigma A(t)$. Thus, the number of nodes in State S decreases by $\sigma A(t)$ in the next hop and $p\sigma A(t)$ out of $\sigma A(t)$ nodes go to State I and $(1-p)\sigma A(t)$ nodes directly change to State R, as shown in Fig. 2. Therefore, corresponding to the differential equations (1), we can obtain the following difference equations with respect to the number of nodes in each state as a function of the hop index t;

$$\begin{cases} S(t) = S(t-1) - \sigma A(t) \\ I(t) = p\sigma A(t) \\ R(t) = R(t-1) + I(t-1) + (1-p)\sigma A(t) \end{cases} \tag{4}$$

with the initial condition (3).

Here, we define the message delivery ratio as the ratio of the number of nodes which gain the broadcast message to the total number of nodes;

$$\eta(t) = \frac{R(t)}{N} \tag{5}$$

for $t = 0,1,2,\ldots$.

C. Evaluation of Area $A(t)$

In order to evaluate the message delivery ratio from (4) and (5), we need to know the area $A(t)$, where nodes just received the broadcast message are dispersed. However, in general, it is considerably complicated to theoretically derive $A(t)$ as a function of t with sufficient accuracy. Related to the evaluation of $A(t)$, an asymptotic and geometrical technique is employed to evaluate asymptotic distributions of the number of isolated nodes in wireless ad hoc networks in [12]. However, we adopt a simple annular dissemination assumption investigated in [10][11] without stepping into precise geometrical techniques. With this assumption, we can suppose that the broadcast message is disseminated annularly hop-by-hop, as shown in Fig. 4. Let $r(t)$ be the distance from the origin where the message can reach at the t th hop. Then, $A(t)$ is the area of an intersection of the square region with side L and the annulus with the outer radius $r(t)$ and the inner radius $r(t-1)$. It is reasonable to suppose that $r(0) = 0$. Apparently, $r(1) = r_0$ and $A(1) = \pi r_0^2$, if $r_0 \le L/2$. It follows that $r(t)$ is an increasing function with respect to t and that $r(t) - r(t-1) \le r_0$, since the transmission range of any node is r_0.

We first derive $A(t)$ as a function of $r(t)$. Then, we mention the evaluation of $r(t)$ in the following subsection. In deriving $A(t)$, we consider three types of an intersection of an annulus and the square region.

1) Annulus is Completely Inside the Square Region

As the first type, consider that an annulus is completely inside the square region. This is true for $r(t) \le L/2$. In this case, it is easily derived that

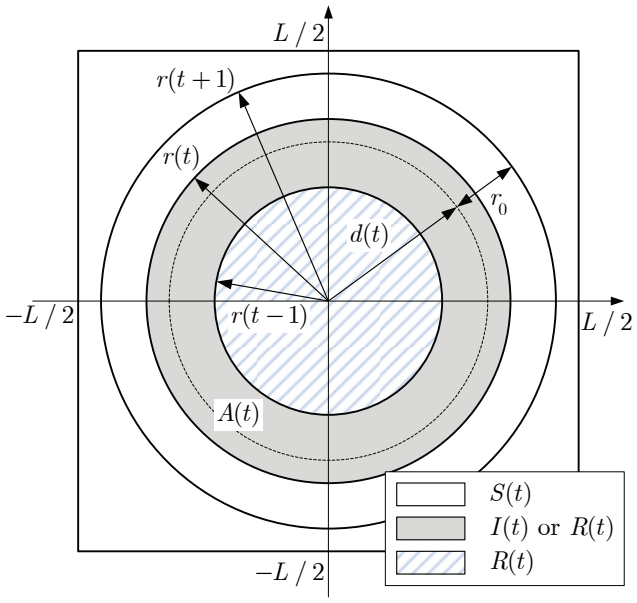

Fig. 4. Annular dissemination of broadcast message.

$$A(t) = \pi[\{r(t)\}^2 - \{r(t-1)\}^2], \tag{6}$$

since $A(t)$ is equal to the area of an annulus with the outer radius $r(t)$ and the inner radius $r(t-1)$, as shown in Fig. 4.

2) Annulus Partially Overlaps with the Square Region

Let us suppose that an annulus partially overlaps the square region. This happens when $r(t) > L/2$ and $r(t-1) < L/\sqrt{2}$. In this case, we can further divide the overlapping type into four cases according to the relation among two radii of the annulus, $r(t)$ and $r(t-1)$, and the side of the square, L, as shown in Fig. 5.

Case 1: For $r(t-1) < L/2 < r(t) \le L/\sqrt{2}$, the outer circle intersects the square and the inner circle is inside the square.

Case 2: For $r(t-1) < L/2$ and $L/\sqrt{2} < r(t)$, the outer

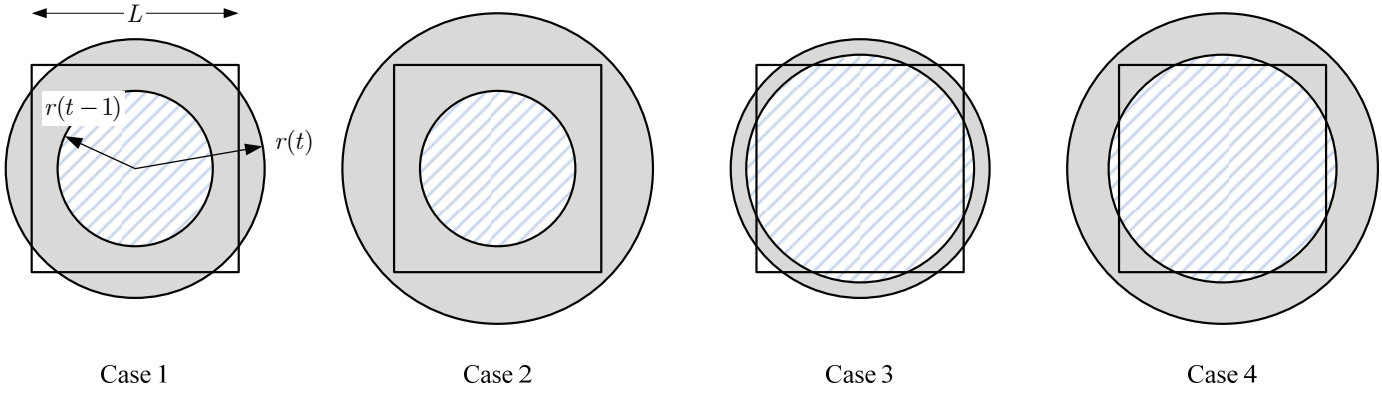

Fig. 5. Four cases according the relation among two circles of the annulus and the square.

circle is outside the square and the inner circle is inside the square.

Case 3: For $L/2 \le r(t-1) < r(t) \le L/\sqrt{2}$, both the outer circle and the inner circle intersect the square.

Case 4: For $L/2 \le r(t-1) < /\sqrt{2} < r(t)$, the outer circle is outside the square and the inner circle intersects inside the square.

For each case, the area $A(t)$ is given by

$$A(t) = \begin{cases} V + g(r(t)) & \text{for Case 1,} \\ L^2 - \pi\{r(t-1)\}^2 & \text{for Case 2,} \\ V + g(r(t)) - g(r(t-1)) & \text{for Case 3,} \\ L^2 - \pi\{r(t-1)\}^2 - g(r(t-1)) & \text{for Case 4,} \end{cases} \tag{7}$$

where

$$V = \pi[\{r(t)\}^2 - \{r(t-1)\}^2], \tag{8}$$

and

$$g(x) = L\sqrt{4x^2 - L^2} - 4x^2 \arccos\frac{L}{2x}. \tag{9}$$

The derivations are given in Appendix.

3) Annulus is Completely Outside the Square Region

As the last type, consider that an annulus is completely outside the square region. This happens when $r(t-1) \ge L/\sqrt{2}$. In this case, it is evident that

$$A(t) = 0, \tag{10}$$

since no intersection appears.

D. Evaluation of Radius $r(t)$

Next, we formulate $r(t)$ in a recursive manner, which is required to evaluate $A(t)$. Nodes which forward the message, or equivalently nodes in State I, are uniformly distributed in the area $A(t)$. If these nodes occasionally happen to be located densely in the vicinity of the outer circle of the annulus, then the message is broadcast furthest. In such a case, the relation $r(t+1) = r(t) + r_0$ holds. To the contrary, if nodes in State I are located in the vicinity of the inner circle of the annulus, then effective message broadcast is not expected, that is, $r(t+1) = r(t) + \varepsilon$ for some small positive value ε.

In order to alleviate the above stated stochastic phenomena, we introduce the concept of the virtual radius $d(t)$. The virtual radius $d(t)$ is a radius where all nodes in State I are assumed to be located on a circle of radius $d(t)$ uniformly at the t th hop. Using $d(t)$, the radius $r(t+1)$ at the next hop can be expressed as

$$r(t+1) = d(t) + r_0, \tag{11}$$

as shown in Fig. 4.

We suppose the following three cases as the virtual radius $d(t)$:

1) Dense Case

Aforementioned, if the node density σ is sufficiently large, the radius $r(t)$ of an annulus increases by the transmission range r_0. Thus, we consider as the first virtual radius;

$$d_{\mathrm{rt}}(t) = r(t). \tag{12}$$

2) Average Case

As the second case of the virtual radius, we focus on the random distribution of nodes in State I in the annulus. The probability distribution function with respect to the distance x between a node in the annulus of the outer radius $r(t)$ and the inner radius $r(t-1)$ and the origin is formulated as

$$F(x) = \frac{\pi x^2 - \pi\{r(t-1)\}^2}{\pi\{r(t)\}^2 - \pi\{r(t-1)\}^2} \tag{13}$$

for $r(t-1) \le x \le r(t)$. The average distance of nodes in the annulus can be evaluated as

$$\begin{aligned} d_{\mathrm{ave}}(t) &= \int_{r(t-1)}^{r(t)} x \cdot \frac{dF(x)}{dx}\, dx \\ &= \frac{2}{3} \cdot \frac{\{r(t)\}^2 + r(t)r(t-1) + \{r(t-1)\}^2}{r(t) + r(t-1)} \end{aligned} \tag{14}$$

We employ $d_{\mathrm{ave}}(t)$ as the second virtual radius.

3) Proposed Exponential Case

The above two virtual radii, $d_{\mathrm{rt}}(t)$ and $d_{\mathrm{ave}}(t)$, are defined independently of the node density σ and the forwarding probability p. However, since the number of nodes in State I is proportional to p, it can be easily expected that $d_{\mathrm{rt}}(t)$ may provide accurate results for sufficiently large $p\sigma$ and that $d_{\mathrm{ave}}(t)$ may be appropriate for moderate $p\sigma$. In order to examine the dependency of the virtual radius of nodes in State I on parameters σ and p, we carry out computer simulation.

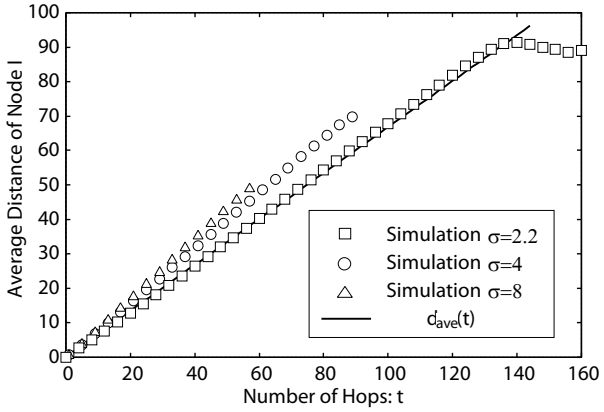

Fig. 6. Average distance of nodes in State I as a function of hop index t for the forwarding probability $p = 1$.

The obtained results of the average distance between nodes in State I and the origin for $p = 1$ are presented as a function of the hop index t in Fig. 6. In Fig. 6, the solid line presents the virtual radius $d_{\text{ave}}(t)$ in (14). From Fig. 6, it can be found that the average distance of nodes in State I increases as the node density σ increases and that the average distance well coincides with $d_{\text{ave}}(t)$ for $\sigma = 2.2$. From these observations, the virtual radius $d(t)$ should satisfy

$$\begin{cases} \lim_{p\sigma\to\infty} d(t) = d_{\text{rt}}(t) \\ \lim_{p\sigma\to 2.2} d(t) = d_{\text{ave}}(t) \\ \lim_{p\sigma\to 0} d(t) = 0 \end{cases} \tag{15}$$

where the last condition corresponds to a trivial case that no message broadcast may occur for extremely sparse node density or for extremely small forwarding probability.

In order to take into account the above examination, we propose to adopt the following exponential function as the virtual radius;

$$d_{\text{prop}}(t) = d_{\text{rt}}(t)\left[1 - \left\{1 - \frac{d_{\text{ave}}(t)}{d_{\text{rt}}(t)}\right\}^{(p\sigma/2.2)^{\alpha}}\right] \tag{16}$$

where α is a design parameter to be calibrated. Illustrative behavior of $d_{\text{prop}}(t)$ is depicted in Fig. 7 as a function of $p\sigma$. It follows from Fig. 7 that for $p\sigma > 2.2$, a large value of α results in large $d_{\text{prop}}(t)$, which implies that for large α, more nodes in State I exist in the vicinity of the outer circle of the annulus, so that it is possible for the message to be broadcast faster. By contrast, a small value of α suppresses fast broadcast and the results approach to the case with the average case of the virtual distance $d_{\text{ave}}(t)$.

IV. Numerical Example

We examine the derived temporal expressions of the message delivery ratio by extensive computer simulation programmed in C language. The results of computer simulation are the average of 2,000 trials.

We consider a network consisting of $N = 40,000$ nodes with transmission range $r_0 = 1$, which are randomly located in a square with side L. The node density $\sigma = 2.0, 4.0, 8.0$ is assumed. The resultant values of side of a square and the average number of neighboring nodes are listed in TABLE I. The forwarding probability is set to $p = 1.0, 0.5$. We calibrate the design parameter α in (16) to $\alpha = 0.21$, which is determined by means of heuristic and exhaustive search for a coincidence with computer simulation results.

The message delivery ratio $\eta(t)$ for the forwarding probability $p = 1.0$ and $p = 0.5$ is shown in Fig. 8 and Fig. 9, respectively. In Fig. 8 and Fig. 9, simulation results are presented by squares and theoretical results based on the virtual radii are shown by lines. Solid lines represent the results using the proposed virtual radius $d_{\text{prop}}(t)$, dashed lines are obtained with $d_{\text{ave}}(t)$, and dotted-dashed lines are the results with $d_{\text{rt}}(t)$. From these six graphs in Fig. 8 and Fig. 9, the theoretical results with the proposed virtual radius $d_{\text{prop}}(t)$ well coincide with simulation results if $p\sigma \geq 2.0$, that is, except for Fig. 9(a). The theoretical results with $d_{\text{rt}}(t)$ increase faster than the simulation results. It implies that much higher node density is required to assume that sufficient forwarding nodes exist in the vicinity of the outer circle of an annulus. By contrast, the results with $d_{\text{ave}}(t)$ provide a slower increase of the message delivery ratio for $p\sigma \geq 4.0$, as shown in Fig. 8(b)(c) and Fig. 9(c). In such cases, more forwarding nodes are located further than the average distance. Notice here that, as shown in Fig. 8(a) and Fig. 9(b) both of which are the results for $p\sigma = 2.0$, the theoretical results with $d_{\text{ave}}(t)$ and $d_{\text{prop}}(t)$ nearly coincide, since $d_{\text{prop}}(t)$ is tuned so as to agree with $d_{\text{ave}}(t)$ for $\sigma = 2.2$ and $p = 1.0$. The graph for $\sigma = 2.0$ and $p = 0.5$ in Fig. 9(a) provides disagreement between the theoretical and simulation results. According to the simulation results, the message is hardly broadcast for $\sigma = 2.0$ and $p = 0.5$. However, the theoretical results exhibit message delivery. To refine the theoretical results, the virtual radius $d_{\text{prop}}(t)$ should be improved for $0 < p\sigma < 2$.

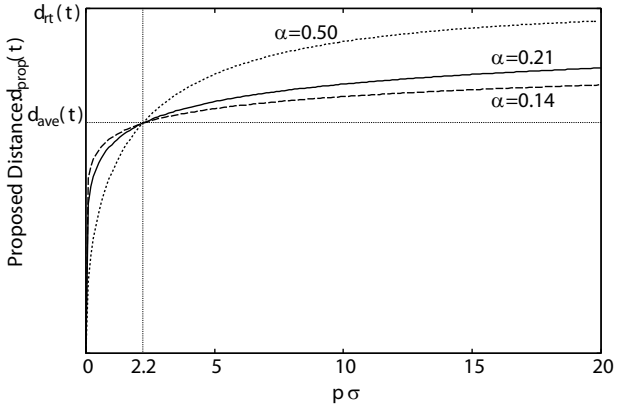

Fig. 7. Illustrative behavior of $d_{\text{prop}}(t)$ as a function of $p\sigma$ for $\alpha = 0.14, 0.21, 0.5$.

TABLE I
VALUES OF PARAMETERS FOR NUMERICAL EXAMPLES

Node Density (σ)	Side of Square (L)	Average Number of Neighbors ($\sigma\pi r_0$)
$\sigma = 2.0$	$L = 141.42$	6.28
$\sigma = 4.0$	$L = 100.00$	12.57
$\sigma = 8.0$	$L = 70.71$	25.13

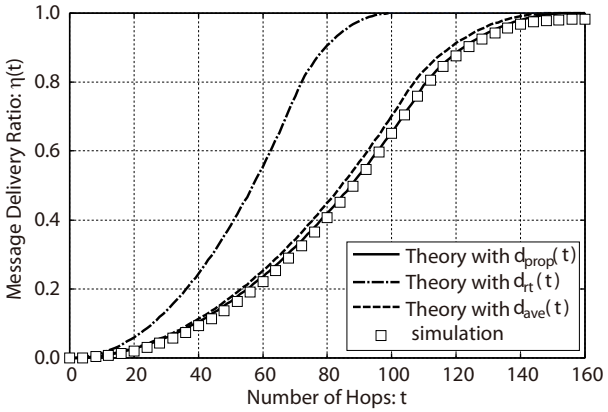

(a) node density $\sigma = 2.0$ ($L = 141.42$) and forwarding probability $p = 1.0$

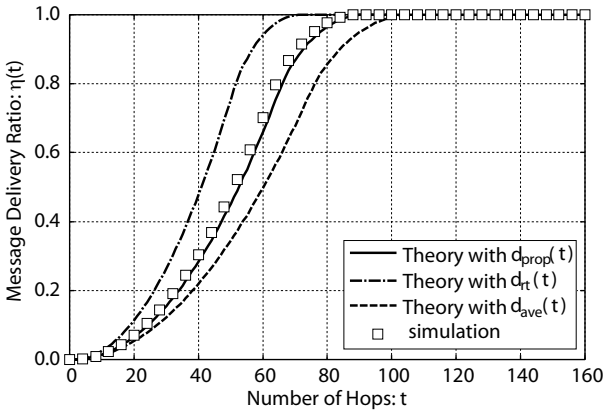

(b) node density $\sigma = 4.0$ ($L = 100.00$) and forwarding probability $p = 1.0$

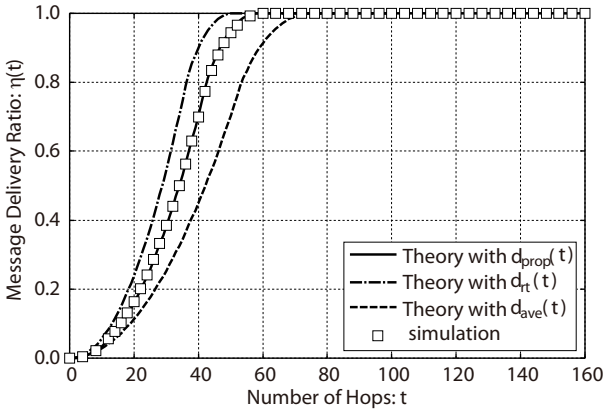

(c) node density $\sigma = 8.0$ ($L = 70.71$) and forwarding probability $p = 1.0$

Fig. 8. Message deliver y ratio for $N = 40,000$ and $p = 1.0$

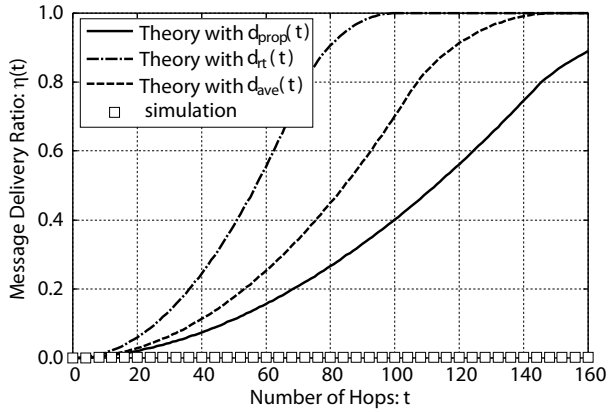

(a) node density $\sigma = 2.0$ ($L = 141.42$) and forwarding probability $p = 0.5$

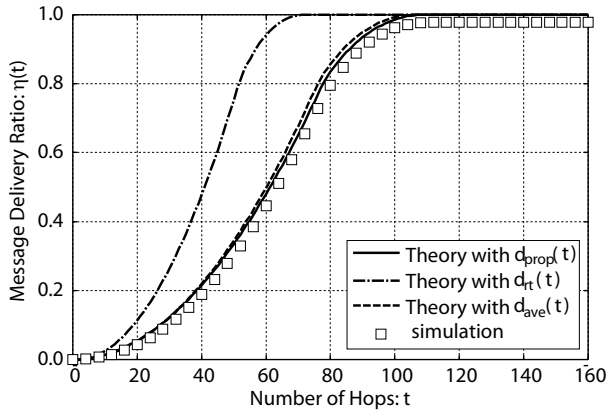

(b) node density $\sigma = 4.0$ ($L = 100.00$) and forwarding probability $p = 0.5$

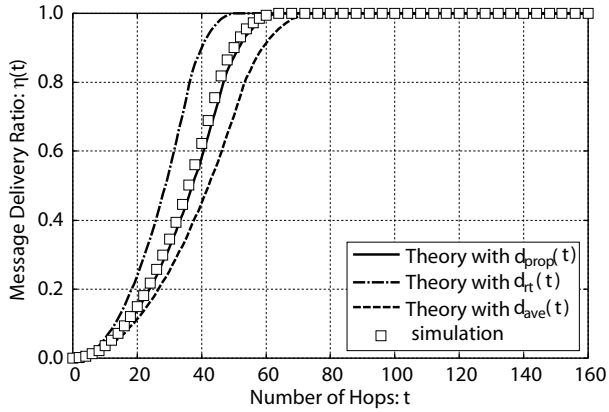

(c) node density $\sigma = 8.0$ ($L = 70.71$) and forwarding probability $p = 0.5$

Fig. 9. Message delivery ratio for $N = 40,000$ and $p = 0.5$

The proposed virtual radius $d_{\text{prop}}(t)$ in (16) indicates larger values for $0 < p\sigma < 2$, which should be smaller.

On this point, the percolation theory offers some insights [13][14]. The percolation theory describes behavior of the connectivity among nodes in a certain graph, such as a square lattice and a random graph. Plain flooding among nodes with identical transmission range can be identified with unit-disc percolation discussed in [14]. In the unit-disc percolation

discussed in [14], a node which are placed in an infinite two-dimensional plane subject to a Poisson point process is assigned to the center of disc of radius r. Then, two nods are connected whenever the distance between the nodes is less than or equal to $2r$. According to the results in [14], the disc percolation occurs when each disc has more than 4.51 neighbors on average, that is, nodes are connected unboundedly. The value 4.51 corresponds to the node density $\sigma = 4.51 / \pi = 1.44$ in our random deployment of nodes. Thus, we can expect that a message may be broadcast to a considerable extend, when $p\sigma > 1.44$. In this sense, a message may not be disseminated for $\sigma = 2.0$ and $p = 0.5$, as shown in Fig. 9(a). This observation implies that the virtual radius should vanish, $d(t) \sim 0$, for $p\sigma < 1.44$ in contrast with Fig. 7.

V. Conclusion

The message delivery ratio of probabilistic flooding has been analyzed for a network with nodes randomly dispersed in a square region. A classical epidemic model, SIR model, has been modified by taking into account the forwarding probability and by introducing the concept of the virtual radius, so that the annular spread assumption can properly describe message dissemination not only in a dense network but also in a moderate-density network. The virtual radius is defined as a function of the hop index with parameters of the node density and the forwarding probability. Extensive computer simulation has been conducted in order to examine the accuracy of the model. Numerical results have indicated that the model is sufficiently accurate, if the product of the node density and the forwarding probability is greater than approximately two.

Further study includes the incorporation of the MAC sub-layer protocol, such as CSMA/CA, and the refinement of the model when the product of the node density and the forwarding probability is less than two.

Appendix
Derivation of (7)

In this auxiliary section, we derive the area $A(t)$ as a function of the radius $r(t)$ in (7).

First, we consider an intersection of a square ACOE with side $L / 2$ and a circular arc of radius x, $L / 2 < x < L / \sqrt{2}$, as shown in Fig. 10. The square corresponds to a upper left quarter square of the square with side L, where nodes are dispersed shown in Fig. 3. Let a vertex O represent the position of the source node. The circular arc centers at O and intersects with the square ACOE at B and F. Let D be an intersection of a diagonal AO and a circular arc.

Consider a triangle ACO. Let $\mathrm{BC} = h$ and $\angle \mathrm{BOD} = \theta$. From Pythagorian theorem,

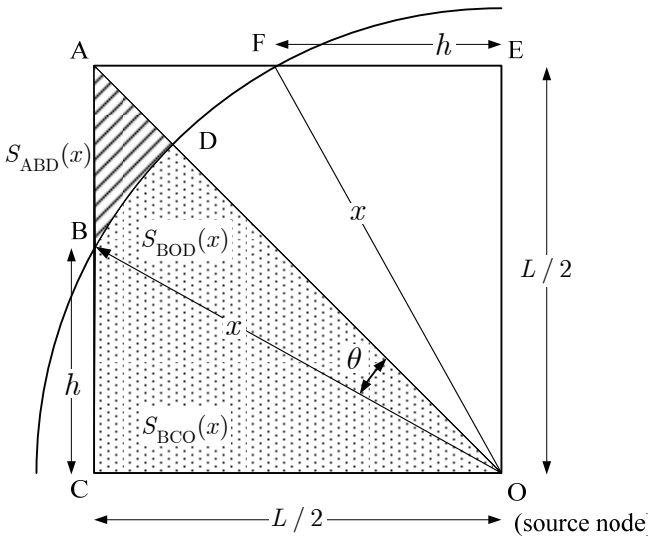

Fig. 10. Intersection of a square and a circular arc.

$$h = \sqrt{x^2 - \left(\frac{L}{2}\right)^2}\,, \tag{17}$$

which provides the area of a triangle BCO as

$$S_{\mathrm{BCO}}(x) = \frac{L}{4}\sqrt{x^2 - \left(\frac{L}{2}\right)^2}\,. \tag{18}$$

Since $\angle \mathrm{AOC} = \angle \mathrm{DOC} = \pi / 4$, we have

$$\theta = \angle \mathrm{AOC} - \angle \mathrm{BOC} = \frac{\pi}{4} - \arccos\frac{L}{2x}\,. \tag{19}$$

Then, the area of a sector BOD is

$$S_{\mathrm{BOD}}(x) = \pi x^2 \cdot \frac{\theta}{2\pi}\,. \tag{20}$$

Hence, the dotted area OCBD in Fig. 10 is given by adding $S_{\mathrm{BCO}}(x)$ and $S_{\mathrm{BOD}}(x)$;

$$S_{\mathrm{OCBD}}(x) = S_{\mathrm{BCO}}(x) + S_{\mathrm{BOD}}(x)\,. \tag{21}$$

The area with slanted lines ABD is given by substituting the dotted area OCBD from a triangle ACO;

$$S_{\mathrm{ABD}}(x) = \frac{1}{2}\left(\frac{L}{2}\right)^2 - S_{\mathrm{OCBD}}(x)\,. \tag{22}$$

With the above preparation, we can derive (7) as follows:

Case 1: As shown in Fig. 5(a), the outer circle of radius $r(t)$ is partially outside the square and the inner circle of radius $r(t-1)$ is inside the square. Thus,

$$\begin{aligned} A(t) &= 8S_{\mathrm{OCBD}}(r(t)) - \pi\{r(t-1)\}^2 \\ &= L^2 - \pi\{r(t-1)\}^2 - 8S_{\mathrm{ABD}}(r(t)) \\ &= V + g(r(t)) \end{aligned} \tag{23}$$

holds, where V and $g(x)$ are defined by (8) and (9), respectively.

Case 2: As shown in Fig. 5(b), the outer circle is completely outside the square and the inner circle completely inside the square. Apparently,

$$A(t) = L^2 - \pi\{r(t-1)\}^2 \tag{24}$$

holds.

Case 3: As shown in Fig. 5(c), both the outer circle and the inner circle intersect the square. We have

$$\begin{aligned} A(t) &= 8\left\{S_{\mathrm{OCBD}}(r(t)) - S_{\mathrm{OCBD}}(r(t-1))\right\} \\ &= V + g(r(t)) - g(r(t-1)). \end{aligned} \tag{25}$$

Case 4: As shown in Fig. 5(d), the outer circle is completely outside the square and the inner circle intersects inside the square. Thus, we can obtain

$$\begin{aligned} A(t) &= 8S_{\mathrm{ABD}}(r(t-1)) \\ &= L^2 - \pi\{r(t-1)\}^2 - g(r(t-1)). \end{aligned} \tag{26}$$

It completes the derivation of (7)

REFERENCES

[1] C.-K. Toh, *Ad Hoc Mobile Wireless Networks: Protocols and Systems*, Prentice Hall, Upper Saddle River, NJ, 2002.

[2] I. Stojmenovic and J.Wu, "Broadcasting and activity scheduling in ad hoc networks," in S. Basagni, M. Conti, S. Giordano and I. Stojmenovic (Eds.), *Mobile Ad Hoc Networking*, IEEE Press, Piscataway, NJ, pp. 205–230, 2004.

[3] J. P. Macker and M. S. Corson, "Mobile ad hoc networks (MANETs): Routing technology for dynamic wireless networking," in S. Basagni, M. Conti, S. Giordano and I. Stojmenovic (Eds.), *Mobile Ad Hoc Networking*, IEEE Press, Piscataway, NJ, pp. 255–273, 2004.

[4] X. Ma, J. Zhang, X. Yin and K. S. Trivedi, "Design and analysis of a robust broadcast scheme for VANET safety-related services," *IEEE Trans. Veh. Tech.*, Vol. 61, No. 1, pp. 46–61, Jan. 2012.

[5] S. Y. Ni, Y. C. Tseng, Y. S. Chen and J. P. Sheu, "The broadcast storm problem in a mobile ad hoc networks," in *Proc. ACM MobiCom '99*, Seattle, WA, pp. 151–162, Aug. 1999.

[6] S. Crisostomo, U. Schilcher, C. Bettstetter and J. Barros, "Probabilistic flooding in stochastic networks: Analysis of global information outreach," *Computer Networks*, vol. 56, no. 1, pp. 142–156, Jan. 2012.

[7] G. Vakulya and G. Simon, "Energy efficient percolation-driven flood routing for large-scale sensor networks," in *Proc. Intl. Multiconf. on Computer Science & Inform Tech. (IMCSIT 2008)*, Wisla, Poland, pp. 877–883, Oct. 2008.

[8] A. Qayyum, L. Viennot, A. Laouiti, "Multipoint relaying for flooding broadcast messages in mobile wireless networks," in *Proc. Hawaii Intl. Conf. Syst. Sci. (HICSS 2002)*, Big Island, HI, pp. 3866–3875, Jan. 2002.

[9] E. Vynnycky and R. G. White, *An Introduction to Infectious Disease Modelling*, Oxford University Press, Oxford, U.K., 2010.

[10] P. De, Y. Liu and S. K. Das, "An epidemic theoretic framework for vulnerability analysis of broadcast protocols in wireless sensor networks," *IEEE Trans. Mobile Computing*, vol. 8, no. 3, pp. 413–425, Mar. 2009.

[11] S. Tang and B. L. Mark, "Analysis of virus spread in wireless sensor networks: An epidemic model," in *Proc. Workshop on Design of Reliable Commun. Networks (DRCN 2009)*, Washington, D.C., pp. 86–91, Oct. 2009.

[12] C.-W. Yi, P.-J. Wan, X.-Y. Li and O. Frieder, "Asymptotic distribution of the number of isolated nodes in wireless ad hoc networks with Bernoulli nodes," *IEEE Trans. Commun.*, vol. 54, no. 3, pp. 510–517, Mar. 2006.

[13] D. Stauffer and A. Aharony, *Introduction to Percolation Theory, 2nd Ed.*, CRC Press, New York, 1994

[14] M. Franceschetti, L. Booth, M. Cook, R. Mee and J. Bruck, "Continuum percolation with unreliable and spread-out connections," *J. Stat. Phy.*, Nol. 118, No. 3/4, pp. 721–734, Feb. 2005.